

# *Herschel*/HIFI CO, $^{13}\text{CO}$ and $\text{H}_2\text{O}$ thermal emission in Water Fountain stars

E. García-García<sup>1,2,3</sup>, J. R. Rizzo<sup>1</sup>, and J. F. Gómez<sup>4</sup>

<sup>1</sup> Centro de Astrobiología (INTA-CSIC), Torrejón de Ardoz, Spain

<sup>2</sup> Univ. Grenoble Alpes, IPAG, F-38000 Grenoble, France

<sup>3</sup> CNRS, IPAG, F-38000 Grenoble, France

<sup>4</sup> Instituto de Astrofísica de Andalucía (CSIC), Granada, Spain

## Abstract

Water fountain stars are low- and intermediate-mass ( $0.8\text{--}8 M_{\odot}$ ) evolved object whose water maser emission trace high velocity ( $> 100 \text{ km s}^{-1}$ ) bipolar jets. They can be found in late AGB phase up to young PNe, although most of them are in the post-AGB phase. These stars may be key objects to understand how planetary nebulae are shaped. Besides the jets, WFs are expected to be surrounded by a large envelope expelled during the AGB and, in some cases, by a circumstellar toroid.

We present a study of thermal lines (mid and high- $J$  CO and  $^{13}\text{CO}$ , and the lowest transitions of  $\text{H}_2\text{O}$ ) from 8 WFs with the *Herschel* Space Observatory, in order to characterise their circumstellar material. The detected lines have been analysed with LTE and LVG models, to obtain the parameters of their circumstellar envelopes. Our results also suggest the presence of thermal emission associated with the outflows. Isotope ratios of CO are compared with those in other post-AGB stars.

## 1 Introduction

The mechanisms that drive the shaping of planetary nebulae are still unclear, although this sculpting probably occurs in the post-AGB phase. There is growing consensus that collimated jets ejected during this phase carve the circumstellar envelope (CSE), and will determine the shape of the future planetary nebulae (PNe). “Water fountain” stars (hereafter WFs), are evolved stars that show a large velocity spread in their 22 GHz water maser emission. These peculiar objects cover an age spread from late AGB [6] to very young planetary nebulae [4], although most of them are in the post-AGB phase [7]. When observed with single-dish observations, the 22 GHz emission can spread from typically  $\geq 75 \text{ km s}^{-1}$  up to  $\simeq 500 \text{ km s}^{-1}$  [3]. Although when using high angular-resolution observations, they display bipolar

collimated jets of water spots that extend between 100 and 500 AU. The short dynamical ages of their outflows ( $<100$  yr [7]) may prove one of the first manifestations of collimated mass-loss in evolved stars. Therefore, WFs may be key objects to understand the transition from spherical AGB to asymmetric PNe [10, 1].

To date only 13 sources have been confirmed as WFs. A possible reason of this low number is the fast evolutionary stage in which they appear.

## 2 Observations

We have carried out a survey of CO,  $^{13}\text{CO}$  mid- and high- $J$  (between  $J=5-4$  and  $J=10-9$ ) and low rotational transitions of  $\text{H}_2\text{O}$  in WFs. This project is a continuation of a previous survey of low- $J$  rotational lines of CO and  $^{13}\text{CO}$  [9]. The general aim of the work is to understand the mechanisms that drive the outflows in WFs, while contributing to the characterisation of their different components, i.e., the CSE expelled in their former AGB phase, outflows and disk/tori around the central star.

The observations were carried out using the HIFI instrument [2] onboard the *Herschel* Space Observatory [8]. Two independent H and V orthogonal polarisations were obtained with the Wide-Band Spectrometer (WBS). The receiver of the heterodyne instrument worked in the double side-band mode (DBS).

We have followed the standard HIFI pipeline to reduce the data (i.e concatenation of sub-bands, average of polarisations, baseline subtraction). Finally, we have exported the observations to CLASS (GILDAS software) to finish the analysis and fitting. JPL and CDMS molecular spectroscopy catalogs were used to identify the positive detections. The final sample comprises a total of 51 HIFI-WBS spectra from 7 different sources. Fourteen lines from 4 different chemical species were positively detected. Table 1 shows a snapshot of all the observations.

Table 1: Rotational transitions observed in WFs.

Source	CO				$^{13}\text{CO}$			CI		$\text{H}_2\text{O}$				
	10-9	7-6	6-5	5-4	10-9	6-5	5-4	2-1	1-0	$3_{21}-3_{12}$	$3_{12}-3_{03}$	$2_{02}-1_{11}$	$1_{10}-1_{01}$	$1_{11}-1_{00}$
I15103	Green	Green		Green			Red	Red	Green			Red	Red	Green
I16342	Green	Green	Green	Red	Green	Green	Green	Grey	Red	Green	Green	Green	Orange	Green
I18043	Red		Orange							Red				
I18286	Red		Green							Red			Red	
I18450	Red		Orange							Grey			Red	
I18460	Red	Green		Red			Red	Red	Green			Red	Red	Red
I18596	Red	Red		Green			Red	Green	Green			Red	Green	Red

Legend. Blank spaces: not observed. Green: positive detections. Red: not detected. Orange: tentative detections. Grey: line detected at velocities different from the star velocity.

### 3 Analysis

We have derived the physical conditions on each source following a standard local thermodynamics equilibrium (LTE) analysis of the positive detections. Excitation temperatures ( $T_{\text{ex}}$ ) were derived from the diagrams of rotational energy levels of the molecules, under the assumption of LTE. Table 2 shows the physical parameters derived from this approach.

Besides the CO and the H<sub>2</sub>O emission, unexpected emission of rare water isotopologues was detected. In particular we report report thermal line emission of *ortho*- and *para*- H<sub>2</sub><sup>17</sup>O and H<sub>2</sub><sup>18</sup>O in IRAS 16342–3814 (Figure 1). The non-LTE (LVG approach) analysis of the data is under development. The results together with the data of the low- $J$  rotational lines in WFs [9], will be presented by Rizzo et al. (in preparation).

Table 2: Physical conditions derived from LTE approach.

IRAS Name	$T_{\text{ex}}$ K	$N_{\text{t}}(\text{CO})^a$ $10^{15} \text{ cm}^{-2}$	mass $10^{-3} M_{\odot}$	$n(\text{H}_2)^b$ $10^3 \text{ cm}^{-3}$	$\dot{M}^c$ $M_{\odot} \text{ yr}^{-1}$	<sup>12</sup> C/ <sup>13</sup> C
15103–5754	143(23) <sup>d</sup>	8.5(2.0)	11(3)	1.7(0.4)	$2.3(0.5) \times 10^{-5}$	–
16342–3814	75(10)	5.6(0.9)	7.3(1.3)	1.0(0.2)	$3.3(0.6) \times 10^{-5}$	1.28
18043–2116	50	10.6(2.1)	14(3)	21(4)	$2.7(0.6) \times 10^{-5}$	–
18286–0959	50	2.2(0.4)	3(1)	450(90)	$1.5(0.3) \times 10^{-6}$	–
18450–0148	50	0.98(0.20)	1.3(0.2)	200(40)	$4.5(0.9) \times 10^{-7}$	–
18460–0151	50	9.2(1.8)	12(2)	18.4(3.8)	$1.3(0.3) \times 10^{-5}$	–
18596+0315	50	8.1(1.6)	11(2)	16.2(3.2)	$6.0(2.1) \times 10^{-6}$	–

<sup>a</sup>CO total column density.

<sup>b</sup>H<sub>2</sub> particle density.

<sup>c</sup>Mass-loss rate

<sup>d</sup>One-sigma errors within parenthesis.

### 4 Conclusions and future work

From our results, we can derive some conclusions for these WFs as a group. First of all, the circumstellar masses obtained are low, compared with previous works on these sources [5, 9]. Furthermore, higher kinetic temperatures are derived, although we note that we have observed higher- $J$  rotational lines, thus tracing warmer gas. It is possible that these transitions of higher energy preferentially trace outflowing gas and/or material close to the central star, rather than the outer, cooler CSE. The detections can be associated either to outflows and/or material close to the central star. Finally, mass-loss rates are also high, compared with the total masses.

Thermal water lines have larger widths (between 35–50 km s<sup>−1</sup>) than the CO thermal emission (between 15–35 km s<sup>−1</sup>). Though this fact must be studied in detail, in general we may associated this emission with the interaction of the outflow and the CSE material. The positive water detections obtained will be compared with observations in other scenarios, i.e.,

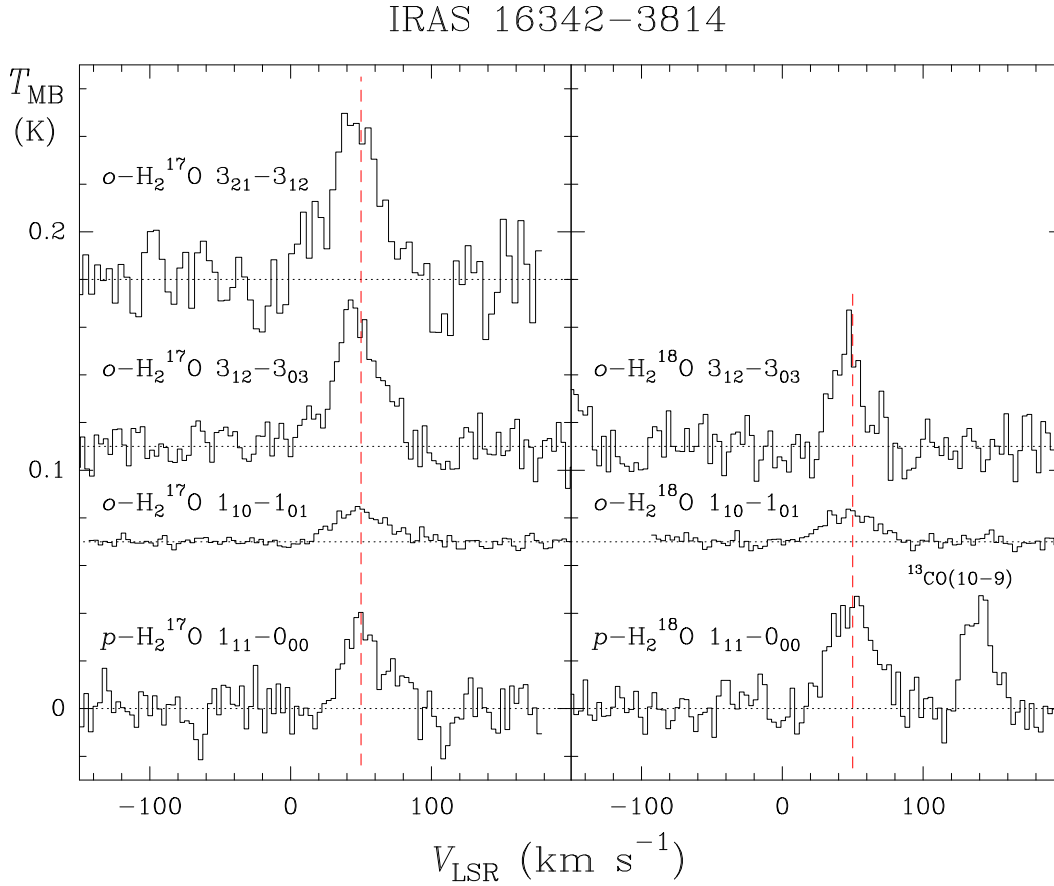


Figure 1: Water isotopologues detected in IRAS 16342–3814. The red dashed vertical line indicates the systemic velocity of the star.

star forming regions and other kinds of evolved stars.

Summing up, we have derived the physical conditions of our sample of WFs under LTE approach, although a deeper analysis is in progress. We note that less than half of our *Herschel* observations were not detected. Furthermore, six known WFs were also not observed. More sensitive data of the undetected sources and lines, together with low- $J$  and interferometric observations will help to create a more general scenario of the WFs, not only of specific sources. Also, derivation and comparison of physical conditions by non-LTE methods will improve the knowledge of how are WFs formed.

## Acknowledgments

J.R.R. acknowledges support from MICINN (Spain) grants CSD2009-00038, AYA2009-07304, and AYA2012-32032. J.F.G is partially supported by grant AYA2011-30228-C03-01 (which includes FEDER funds).

## References

- [1] Bujarrabal, V., Castro-Carrizo, A., Alcolea, J., et al. 2001, *A&A*, 377, 868
- [2] de Graauw, T., Helmich, F. P., Phillips, T. G., et al. 2010, *A&A*, 518, L6
- [3] Gómez, J. F., Rizzo, J. R., Suárez, O., et al. 2011, *ApJ*, 739, L14
- [4] Gómez, J. F., Suárez, O., Bendjoya, P., et al. 2014, *ApJ*, in press
- [5] He, J. H., Imai, H., Hasegawa, T. I., et al. 2008, *A&A*, 488, L21
- [6] Imai, H., Nakashima, J.-i., Diamond, P. J., et al. 2005, *ApJ*, 622, L125
- [7] Imai, H. 2007, *IAU Symposium*, 242, 279
- [8] Pilbratt, G. L., Riedinger, J. R., Passvogel, T., et al. 2010, *A&A*, 518, L1
- [9] Rizzo, J. R., Gómez, J. F., Miranda, L. F., et al. 2013, *A&A*, 560, A82
- [10] Sahai, R., & Trauger, J. T. 1998, *AJ*, 116, 1357